Comunicaciones del CIMAT

SHORTEST PATHS FOR DIFFERENTIAL DRIVE ROBOTS
UNDER VISIBILITY AND SENSOR CONSTRAINTS

Jean- Bernard Hayet, Claudia Esteves and Rafael Murrieta-Cid

CIMAT

Shortest paths for differential drive robots under visibility and sensor constraints

Jean-Bernard Hayet
Center for Mathematical Research
S/N Callejon Jalisco
A.P. 402, Guanajuato Gto., Mexico
jbhayet@cimat.mx

Claudia Esteves
Department of Mathematics
U. of Guanajuato
S/N Callejon Jalisco
Guanajuato Gto., Mexico
cesteves@cimat.mx

Rafael Murrieta-Cid
Center for Mathematical Research
S/N Callejon Jalisco
A.P. 402, Guanajuato Gto., Mexico
murrieta@cimat.mx

Abstract— **This article revisits the problem of planning shortest paths in terms of distance in the plane (i.e., not in time) for the differential drive robot (DDR) in the absence of obstacles. We complete the existing works by explaining and deepening the remarks made recently in the literature [10] that exhibited more cases that what was thought until then. Motivated by that work, we show that there cannot have more than 4-word trajectories and finally exhibit a complete partition of the plane in terms of the nature of the shortest path.**

I. INTRODUCTION

This work aims at a better understanding of the geometrical properties of the shortest paths for a differential drive robot (DDR), placed under the constraints that it has to maintain some landmark in sight, whereas it cannot move its sensor as far as it wants. An example of this situation is a mobile robot equipped with a camera, that has to keep looking at some interesting point whereas the camera has a pan degree of freedom limited to a given angle.

A. Related work

Motion planning with nonholonomic constraints has been a very active research field, and its most important results have been obtained by addressing the problem with tools from differential geometry and control theory. Laumond pioneered this research and produced the result that a free path for a holonomic robot moving among obstacles in a 2D workspace can always be transformed into a feasible path for a nonholonomic car-like robot by making car maneuvers [7].

Inside the planning area, the study of optimal paths for nonholonomic systems has been very active. Reeds and Shepp determined the shortest paths for a car-like robot that can move forward and backward [9]. In [11] a complete characterization of the shortest paths for a car-like robot is given. As for the DDR, in [1], the time-optimal trajectories are determined using the Pontryagin Maximum Principle and geometric analysis, whereas in [4], the PMP is used to obtain the trajectories that minimize the amount of wheel rotation.

The problem of detecting and tracking visual landmarks is a very frequent one in mobile robotics [3], [12], [5], so that

it may be surprising that little attention has been paid to incorporating sensing constraints into motion planning. Among the first works in this area are the ones of Bhattacharya [2] upon which we inspire ours. They study the shortest paths in terms of distance in the plane for DDRs under visibility and sensor constraints, without obstacles. Later, these works were used in the context of visual servoing [8] and extended to handle the case of an environment populated with obstacles [6].

B. Contributions

The main result of this article is to complement the partition of the plane for the DDR under visibility and sensor constraints in terms of the nature of the optimal path. We show that in addition of the $2-$ and $3-$letter trajectories, we may have to consider $3-$ and $4-$letter trajectories of a certain type, and that there cannot have trajectories made of a larger number of path primitives. This article is organized as follows: first, we describe the problem in Section II and complete the nomenclature of possible shortest paths; section III focuses on the $3-$letter optimal paths alone and studies their spatial distribution; finally, section IV studies the case of $4-$letter optimal paths.

C. The differential drive robot

The DDR is described in Fig. 1. It is controlled through commands to its two wheels, i.e. the angular velocities w_l and w_r. Parameters for its control are (1) the distance D from the axis center to each wheel and (2) the radius R of the wheels. Without loss of generality we suppose, in the remaining of this work, that these two quantities are unitary.

We make the usual assignment of a body-attached $x'y'$ frame to the robot. The origin is at the midpoint between the two wheels, y'-axis parallel to the axle, and the x'-axis pointing forward, parallel to the robot heading. The angle θ is the angle formed by the world x-axis and the robot x'-axis. The robot can move forward and backward. Its heading is defined as the direction in which the robot

moves, so the heading angle with respect to the robot x'-axis is zero (forward move) or π (backward move). The position of the robot w.r.t. the origin will be defined either in terms of Cartesian coordinates (x, y) or in terms of polar coordinates $(r, \alpha) : r = \sqrt{x^2 + y^2}$, $\alpha = \arctan \frac{y}{x}$.

The robot is equipped with a pan-controllable sensor with limited field of view (e.g., a camera), that can move w.r.t. the robot basis. We will suppose that this sensor is placed on the robot so that the optical center always lies directly above the origin of the robot's local coordinate frame, i.e., the center of rotation of the sensor is also the one of the robot. Its pan angle ϕ is the angle from the robot x'-axis to its optical axis, and it is limited : $\phi \in [\phi_1, \phi_2]$. We will assume in the remainder that the robot moves in the free space (without physical obstacles) and that $\phi_1 = -\phi_2$, which corresponds to the most realistic case in practice. We will call such a system of a DDR robot with visibility and sensor constraints a V-DDR.
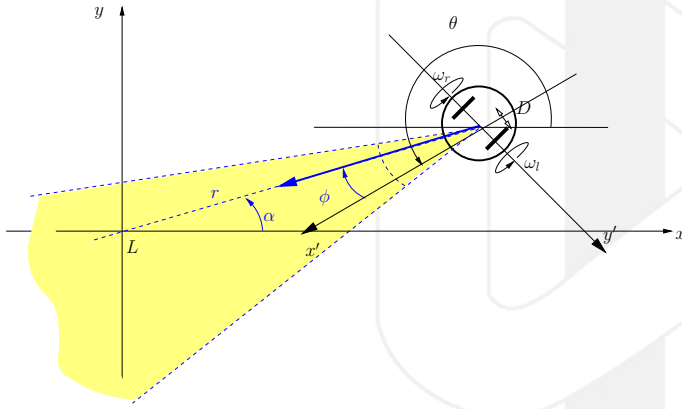

Fig. 1. DDR with visibility constraints under sensor restrictions in angle. The robot visibility region is the shaded region.

II. HANDLING THE SENSOR ANGULAR CONSTRAINTS

In this section, we formalize the angular constraints for the V-DDR, revisit the main properties of shortest paths, and explain why it is possible as in [10] to exhibit examples of 3-letter trajectories that are actually shorter than the shortest 2-letter trajectory. A "letter" in this context has to be understood as a type of motion primitive.

A. Angular constraints

The robot has to maintain in sight a static landmark L located at the origin of the coordinate system, i.e. a clear line of sight, lying within the minimal and maximal bounds of the sensor angle, can join the landmark and the sensor. These constraints can be written as

$$\theta = \alpha - \phi + (2k+1)\pi, \; k \in \mathbb{Z}, \quad (1)$$
$$-\phi_2 \leq \phi \leq \phi_2, . \quad (2)$$

The robot can be seen as living in the special euclidean group $SE(2)$, as from Eq. 1, ϕ is not really a degree of freedom. Moreover, Eqs. 1 and 2 can be rewritten as

$$-\phi_2 \leq -\theta + \arctan(\frac{y}{x}) + (2k+1)\pi \leq \phi_2 \text{ for some } k \in \mathbb{Z}. \quad (3)$$

B. Characterization of shortest paths

Shortest paths for the V-DDR have been studied in [2], from a geometric point of view, and we will use some of its main results. In particular, the motion primitives were shown to be either line segments or arcs of logarithmic spirals, with a countable set of non-differentiable points.
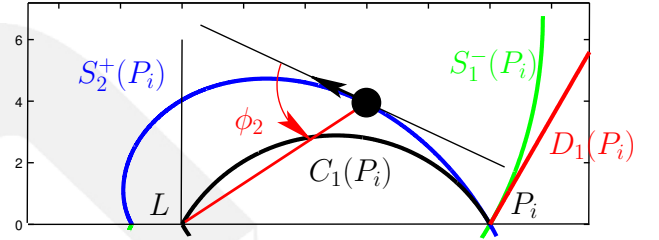

Fig. 2. Critical curves for the study of optimal paths of the V-DDR, around the initial point P_i and the landmark L. The S_1 and S_2 spirals are depicted in green and blue, respectively. The arc of circle C_1 delimits the area of points reachable forwards, along a straight line from P_i.

Let us define P_i as the initial position of the DDR, located, without loss of generality, on the x axis, at a distance r_0 from the landmark L. As depicted on Fig. 2, one can define at P_i two logarithmic spirals $S_1(P_i)$ and $S_2(P_i)$, that appear through Eq. 3 as the trajectories done by the V-DDR while keeping the sensor angle at a saturated value ($\phi = -\phi_2$ or $\phi = \phi_2$). When necessary, we may refer to other S_2 (resp. S_1) spirals through other points P as $S_2(P)$ (resp. $S_1(P)$). The equation of the logarithmic spiral $S_2(P_i)$ is given by

$$r = r_0 e^{-\frac{\alpha}{t_2}},$$

where $t_2 = \tan \phi_2$, and the polar angle α varies in $[-\pi, \pi]$. The $\alpha > 0$ (resp. $\alpha < 0$) part, referred to as $S_2^+(P_i)$ (resp. $S_2^-(P_i)$), is travelled forwards (resp. backwards). We will denote by $\bar{X}$ the symmetric of a curve X w.r.t. the x axis.

Other critical curves, depicted on Fig. 2, are the arcs of circles $C_1(P_i)$ (resp. $\bar{C}_1(P_i)$) passing through P_i and L and tangent to $S_2(P_i)$ (resp. $S_1(P_i)$) at P_i. One can prove [2] that they are the loci of the final points reached from P_i along straight lines before saturation of the sensor angle. The following properties were stated in [2]:

1) optimal paths from P_i to P_f never cross the line LP_i;
2) the points P_f attainable with a straight line, forwards (resp. backwards) motion from P_i are the ones comprised between the arcs $C_1(P_i)$ and $\bar{C}_1(P_i)$ (resp. the half-lines $D_1(P_i)$ and $\bar{D}_1(P_i)$, as depicted in Fig. 2;
3) the optimal paths are necessarily made of arcs of spirals, in-site rotations (at non-differentiable points of the curve) and line segments; we will use the capital letters D, S_1 and S_2 to refer to each local primitive; to denote trajectories, we will use "$-$" to indicate smooth transitions between primitives and "$*$" to indicate non-differentiable transition points; for example, $D - S_1 * S_2$

is a trajectory made of a straight line segment, then, a S_1 spiral has the line as a tangent at the transition point, then a S_2 spiral that connects to the S_1 one at a non differentiable point;

4) the non-differentiable points on optimal paths are necessarily of the type $S_1^- * S_2^-$ or $S_1^+ * S_2^+$ (in any order).

Proof: The proofs for properties 2, 3, 4 can be found in [2]. As for property 1, the proof in [2] says that if the optimal path crosses the line LP_i between P_i and L at some point Q, then it could be shortened by traveling on a straight line between P and Q, as illustrated (in red) in Fig. 3, which would contradict optimality. However, as depicted in the same figure, the DDR may also go *round the landmark* (in green), and cross the line P_iL at some point R, while the path could not be made shorter. When $\phi_1 \neq -\phi_2$, this situation may occur. Now, because our system is symmetric ($\phi_1 = -\phi_2$), the property 1 holds: By symmetry, there is also an optimal (dashed) path from P_i to R that goes on the same side of the x axis as P_f. The resulting trajectory from P_i to P_f would also be optimal. Now, because of property 3, the original trajectory at R is necessarily a line segment or an arc of spiral. Hence, the differential point would be either of the type $D_1 * D_2$, $S_1^- * S_2^+$ or $S_1^+ * S_2^-$, which would contradict Property 4. ∎
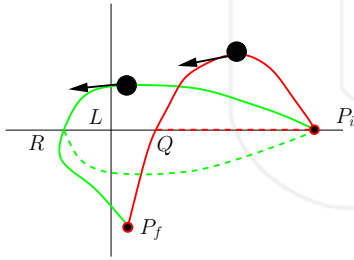

Fig. 3. Illustration for property one: By symmetry, optimal paths cannot cross the horizontal axis.

From this local characterization, the trajectories have been stated to be made of $1-$letter or $2-$letter words, e.g., D-S_1, S_1-D, D, or $S_1 * S_2$ [2]. From the exhaustive characterization of trajectories as words in this alphabet, a partition of the plane was given, according to the nature of the shortest path from P_i to the considered point in the plane, as depicted in Fig. 5. In [10], Salaris et al. have exhibited a configuration that contradicts this partition. They give an example similar to the one depicted in Fig. 4(a): the $2-$letter $S_2 * S_1$ trajectory (in green) should be the shortest one, however the $D - S_2 * S_1$ trajectory (in red) is numerically shown to be shorter.

Such a problem arises because the lemma 1 in [2] discards the words like $D - S_2 * S_1$, whereas it should not. The argument used to discard these words is illustrated in Fig. 4(b). A first potential optimal path starts at P_i and follows a straight line up to M_1, then a S_2 spiral up to Q_1, then reaches P_f on a S_1 spiral. This path could be shortened in another $D - S_2 * S_1$ path that would go through M_2 and Q_2, then the same would apply to get another one through M_3 and Q_3, and so on. At the limit, the optimal path would collapse on a $D * S_2$ path going through W that would invalidate property 4. The

problem is that the iterative shortening of the $D - S_2 * S_1$ paths as explained above is *not always possible*. It would suppose that the path length is a monotonically decreasing function of the polar angle of points M_k, which is not the case, as we will see in next Section. As a consequence, the word $D - S_2 * S_1$, for example, *should* be considered as a candidate for shortest path.

C. Admissible words

A direct consequence of the previous remark is that the vocabulary of admissible words for shortest paths is richer than first expected, as we state it in the next lemma.

Lemma 1: Among the set of shortest paths in the plane, there can be no more than $4-$letter words, and the only $3-$ and $4-$letter trajectories that can be considered for optimality are $D - S_1 * S_2$, $D - S_2 * S_1$, $S_2 * S_1 - D$, $S_1 * S_2 - D$, $D - S_2 * S_1 - D$, and $D - S_1 * S_2 - D$.

Proof: The admissible $1-$ and $2-$letter words have been described in [2], and are recalled in the first two lines of Table I. The authors showed two results onto which we will rely: (i) that given a $S_1 * S_2$ path, no succession of $S_1 * S_2 * S_1 \ldots$ nor $S_2 * S_1 * S_2 \ldots$ could be shorter and (ii) $3-$letter words other than the $D - S_1 * S_2$-like have to be discarded. The last result means that 3-letter combinations $D - S_1 - D$, $D - S_2 - D$, $S_1 - D - S_2$, $S_2 - D - S_1$, $S_2 - D - S_2$ and $S_1 - D - S_1$ are impossible. We deduce that the only possible 3-letter words are $D - S_1 * S_2$, $D - S_2 * S_1$, $S_2 * S_1 - D$, $S_1 * S_2 - D$ (i.e., cases 7 and 8 in [2]).

Now, as shortest paths have an optimal sub-structure, a $4-$letter word includes in it one of the possible $3-$letter words. Because of the limited set of possible transitions ($D - S_1$, $S_1 * S_2$, $\ldots$), this leaves only two possible words : $D - S_2 * S_1 - D$, and $D - S_1 * S_2 - D$. For example, $S_2 * S_1 * S_2 - D$ cannot be optimal since paths with three or more consecutive spirals can be shortened with two spirals only.

The same argument can be used for trajectories made of more than 4 words. Such words cannot be optimal since they would necessarily include one of the two possible $4-$letter sub-word, which by essence cannot be "augmented". They all terminate or start with a line segment, preceded by an arc of spiral, and adding a spiral would contradict the fact that the only possible three-letter words are the ones mentioned above, while adding another straight line would introduce a transition $D * D$ which is not authorized. Hence, no word can be made of more than four letters. ∎

N. of letters	Admissible words
1	D, S_1, S_2
2	$D - S_1$, $D - S_2$, $S_1 - D$, $S_2 - D$, $S_1 * S_2$, $S_2 * S_1$
3	$D - S_1 * S_2$, $D - S_2 * S_1$, $S_2 * S_1 - D$, $S_1 * S_2 - D$
4	$D - S_2 * S_1 - D$, $D - S_1 * S_2 - D$

TABLE I

NOMENCLATURE OF THE ADMISSIBLE WORDS.

The nomenclature of optimal trajectories is described in Table I, adding 6 new words to the already known ones. Next
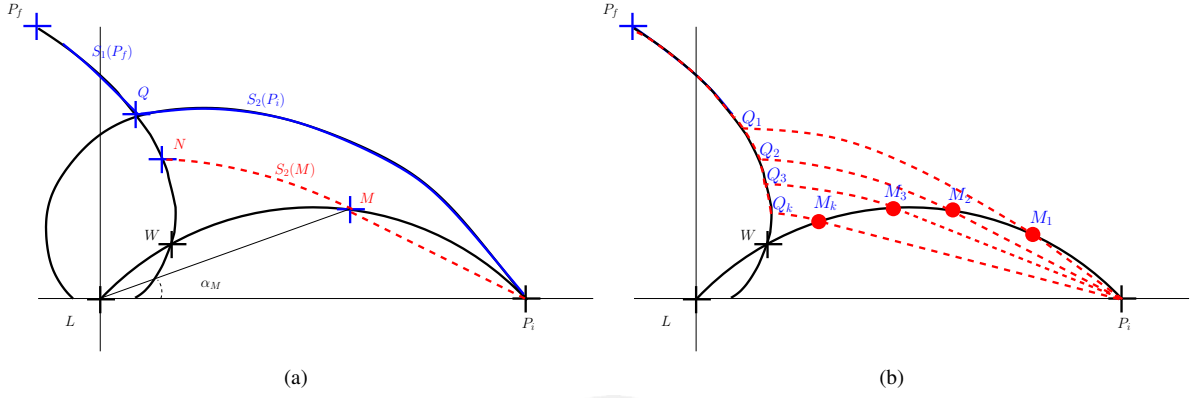
Fig. 4. In (a), configuration in which a 3−letter word gives a shorter path than the shortest path predicted by [2]. The predicted optimal path is made of the $S_2(P_i)$ spiral, that connects to the $S_1(P_f)$ spiral at Q. However, the $D - S_2 * S_1$ trajectory in red is shorter. In (b), the argument in [2] to discard $D - S_2 * S_1$ paths is depicted, stating that $P_i - M_1 - Q_1 - P_f$ can be shortened in $P_i - M_2 - Q_2 - P_f$, then in $P_i - M_3 - Q_3 - P_f$, …and would collapse in $P_i - W - P_f$ which has a non-allowed non-differentiable point.

sections study the conditions under which these new words may generate shorter paths than the already known ones. Our methodology is progressive: first, we sistematically study in each region of the partition from [2], the spatial distribution of 3−letter words, one possible word at a time; second, we compare the 3−letter words (in terms of shorter lengths) one against each other; then, we study the spatial distribution of 4−letter words and finally deduce the complete partition of the plane.

III. THREE-LETTER WORDS AS OPTIMAL PATHS

In this section, we will focus on the 3−letter word $w = D - S_2 * S_1$. We recall the spatial distribution of shortest paths of up to 2 letters and examine in which areas the trajectories made according to w, i.e. w−trajectories, can be shorter.

A. Distribution of the 1−, 2−, and 3− letter optimal paths

If we consider only paths made of up to 2 letters, then the spatial distribution of shortest paths is the one of Fig. 5, extensively described in [2]. There are eight regions, some of them symmetric to others, so that there is in fact only three types of them : D (dark grey regions), $S * S$ (light gray), and $D - S$ (white). The following lemmas give bounds on the areas in which the w-trajectories can be the shortest ones.

Lemma 2: The points of the plane reachable optimally by a trajectory following the word $w = D - S_2 * S_1$ necessarily belong to regions II and IV.

Proof: First notice that w cannot be an optimal path to reach points located in the half-space below the line P_iL: we showed that all optimal trajectories remain in the same half-space; moreover, if the straight line D is travelled in the lower half-space, the sensor angle has to be negative, so that a smooth transition with a S_2 spiral is not possible. Regions II', III' and IV' cannot be reached this way. Moreover, in regions I and I', the shortest paths are straight lines, so they cannot be w-trajectories. Now refer to Figs. 2 and 4(a): by construction, within any w−trajectory, point N (the intersection of the two spirals) will be located below the spiral $S_1^-(P_i)$. As a consequence, the terminating spiral

$S_1^-(P_f)$ can reach only the points located below $S_1^-(P_i)$. Hence, points P_f can only belong to regions II and IV. ∎

Lemma 3: In regions II and IV, any point can be reached through a trajectory following the word $w = D - S_2 * S_1$.

Proof: The proof is constructive. Refer to Fig. 4 (a): for any point P_f in regions II and IV, the point W, intersection of $C_1(P_i)$ and of $S_1(P_f)$, is guaranteed to exist. Then, choose any point M on $C_1(P_i)$ between P_i and W, and build the trajectory $P_i - M - N - P_f$ as in Fig. 4(a). ∎

B. Families of w-trajectories in region IV

Let us consider particularly region IV. The w-trajectories are made according to Fig. 4(a). The point Q, intersection of $S_1(P_f)$ through $P_f = (r_f, \alpha_f)$ and of $S_2(P_i)$, satisfies

$$r_0 e^{-\frac{\alpha_Q}{t_2}} = r_f e^{\frac{\alpha_Q - \alpha_f}{t_2}},$$

which leads to $Q = (r_0^{\frac{1}{2}} r_f^{\frac{1}{2}} e^{\frac{\alpha_f}{2t_2}}, \frac{t_2}{2} \log(\frac{r_0}{r_f}) + \frac{1}{2}\alpha_f)$.

Now consider the family of w trajectories that connect P_i to P_f. To define such a trajectory, you may consider any point M on the circle $C_1(P_i)$. More precisely, if you want this trajectory to be optimal you may consider any M between P and W, intersection of $C_1(P_i)$ with $S_1(P_f)$. Indeed, for points M located between W and L, the trajectory would have to go twice through W, which would not be optimal.

Let (r_M, α_M) be the polar coordinates of point M. The equation of the circle $C_1(P_i)$ can be written as

$$r(r + r_0 \frac{\sin(\alpha - \phi_2)}{\sin \phi_2}) = 0.$$

Hence, the coordinates of M are

$$M = (r_0 \frac{\sin(\phi_2 - \alpha_M)}{\sin \phi_2}, \alpha_M).$$

Let us make of α_M the parameterization of the w-trajectories going from P_i to P_f. The intersection between the two spirals $S_1^-(P_f)$ and $S_2^+(M)$ is N. As it belongs to the S_2 spiral through M,
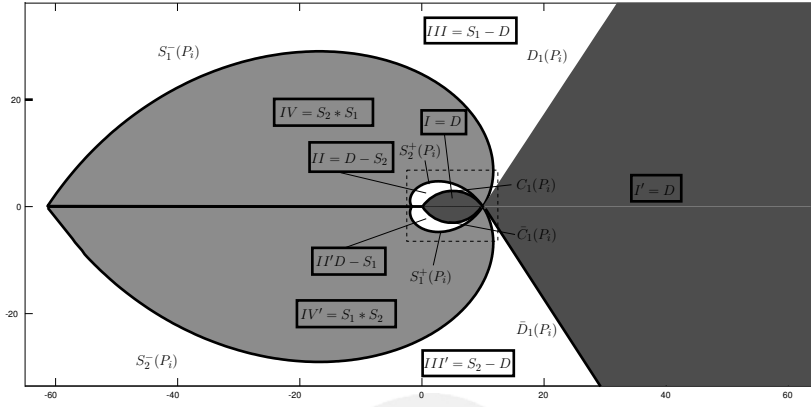
Fig. 5. Distribution of the $1-$ and $2-$letter optimal paths according to the position of P_f in the plane, for $r_0 = 10$ and $\phi_2 = \frac{\pi}{3}$. The dashed rectangle corresponds to the zone depicted in Fig. 2. Capital letters stand for critical curves, framed capital letters stand for particular regions.

$$r_N = r_M e^{\frac{\alpha_M - \alpha_N}{t_2}} = \frac{r_0}{\sin \phi_2} \sin(\phi_2 - \alpha_M) e^{\frac{\alpha_M - \alpha_N}{t_2}}. \quad (4)$$

Point N also belongs to the S_1 spiral going P_f, so that

$$r_N = r_f e^{\frac{\alpha_N - \alpha_f}{t_2}}. \quad (5)$$

By combining Eqs. 4 and 5,

$$r_f e^{\frac{\alpha_N - \alpha_f}{t_2}} = \frac{r_0}{\sin \phi_2} \sin(\phi_2 - \alpha_M) e^{\frac{\alpha_M - \alpha_N}{t_2}},$$

so that, finally,

$$\alpha_N = \frac{t_2}{2} \ln\left(\frac{r_0 \sin(\phi_2 - \alpha_M)}{r_f \sin \phi_2}\right) + \frac{\alpha_f + \alpha_M}{2}.$$

Note that all these derivations imply $\alpha_M < \phi_2$ (which is respected by definition of $C_1(P_i)$). Now let us recall that along a ϕ_i spiral ($i = 1, 2$), the path length between two points A and B is given by $\frac{|r_A - r_B|}{\cos \phi_i}$. We can separate the trajectory into its three parts and compute the length of each,

$$\begin{cases} P_i M &= \frac{r_0 \sin \alpha_M}{\sin \phi_2} \\ MN &= \frac{1}{\cos \phi_2}(r_M - r_N) \\ NF &= \frac{1}{\cos \phi_2}(r_f - r_N), \end{cases}$$

so that the total length of the w-trajectory, $l(\alpha_M)$, parametrized by α_M, sums these quantities into

$$l(\alpha_M) = \frac{r_f}{\cos \phi_2} + \frac{r_0 \sin \alpha_M}{\sin \phi_2} + \frac{1}{\cos \phi_2}(r_M(\alpha_M) - 2r_N(\alpha_M)),$$

and after more developments,

$$l(\alpha_M) = \frac{r_f}{\cos \phi_2} + r_0 \frac{\cos \alpha_M}{\cos \phi_2} - \frac{2}{\cos \phi_2} r_N(\alpha_M). \quad (6)$$

Remark that for $\alpha_M = 0$, N and Q coincide, and P_i and M also coincide, i.e. we are in the case of a $S_2 * S_1$ trajectory.

Now let us look for the minimum value of this function for varying values of α_M. The derivative of $l(\alpha_M)$ is

$$l'(\alpha_M) = -\frac{r_0 \sin \alpha_M}{\cos \phi_2} - \frac{2}{\cos \phi_2} r_N'(\alpha_M).$$

From the expressions of r_N and α_N, we get

$$r_N(\alpha_M) = \sqrt{\frac{r_0 r_f \sin(\phi_2 - \alpha_M)}{\sin \phi_2}} e^{\frac{\alpha_M - \alpha_F}{2t_2}}. \quad (7)$$

After some algebraic developments,

$$r_N'(\alpha_M) = -\frac{\sin \alpha_M}{2} \sqrt{\frac{r_0 r_f}{\sin^3 \phi_2 \sin(\phi_2 - \alpha_M)}} e^{\frac{\alpha_M - \alpha_F}{2t_2}}.$$

Now by substituing into $l'(\alpha_M)$,

$$l'(\alpha_M) = -\frac{r_0 \sin \alpha_M}{\cos \phi_2}\left(1 - \sqrt{\frac{r_f e^{\frac{\alpha_M - \alpha_F}{t_2}}}{r_0 \sin(\phi_2 - \alpha_M) \sin^3 \phi_2}}\right).$$

Vanishing the derivative leads to

$$\frac{r_0}{r_f} \sin^3 \phi_2 e^{\frac{\alpha_f}{t_2}} = \frac{1}{\sin(\phi_2 - \alpha_M)} e^{\frac{\alpha_M}{t_2}}.$$

If we define

$$g(x) = \frac{e^{\frac{x - \alpha_f}{t_2}}}{\sin^3 \phi_2 \sin(\phi_2 - x)},$$

the previous equation becomes

$$g(\alpha_M) = \frac{r_0}{r_f}. \quad (8)$$

Hence, through Eq. 8, for a given P_f, we have a necessary and sufficient condition to get an extremal value for $0 < \alpha_M < \alpha_W$ (i.e., a w-trajectory made of 3 letters). Observe that the function $g(\alpha_M)$ is strictly increasing on $[0, \alpha_W]$ and that its value at 0 is $\frac{e^{-\alpha_f / t_2}}{\sin^4 \phi_2}$. Also observe that point W is the intersection between the arc of circle $C_1(P_i)$ with $S_1(P_f)$. Its coordinates can be shown as satisfying,

$$\frac{e^{\frac{\alpha_W - \alpha_f}{t_2}}}{\sin(\alpha_2 - \phi_W)} = \sin^3 \phi_2 g(\alpha_W) = \frac{r_0}{r_f \sin \phi_2},$$

so that Eq. 8 can be simply rewritten as

$$h(\alpha_M) = \sin^4 \phi_2, \quad (9)$$

where $h(x) = g(x)/g(\alpha_W)$. Based on Eq. 9, and because $h(\alpha_W) = 1$ and h is strictly increasing, we deduce that such an α_M does exist if and only if $h(0) < \sin^4 \phi_2$, in which case it is unique. As a consequence, we have two situations

1) $h(0) > \sin^4 \phi_2$, $l(\alpha_M)$ increases monotically on $]0, \alpha_W]$, and the shortest path is done along $S_2 * S_1$;
2) $h(0) < \sin^4 \phi_2$, $l(\alpha_M)$ decreases down to a minimum point given by Eq. 8, then increases. This point corresponds to the shortest path, done along a w-trajectory.

From this development, we can deduce the following theorem characterizing the part of region IV in which the choice of a $w-$trajectory is better than the choice of a $S_2 * S_1$ trajectory.

Theorem 1: In region IV, a $w-$trajectory is shorter than a $S_2 * S_1$ trajectory if and only if the final point is below the spiral $S_1^-(P_r)$, $r = r_0 \sin^4 \phi_2 e^{\frac{\alpha}{t_2}}$, for $P_r = (r_0 \sin^4 \phi_2, 0)$.

Proof: As shown above, the necessary and sufficient condition is $h(0) < \sin^4 \phi_2$. As $h(0) = \frac{1}{\sin \phi_2} \frac{r_f \sin \phi_2}{r_0} e^{\frac{-\alpha_f}{t_2}}$, we get

$$r_f < r_0 \sin^4 \phi_2 e^{\frac{\alpha_f}{t_2}}. \tag{10}$$

This spiral saturates the sensor at $-\phi_2$, and passes through the point $P_r = (r_0 \sin^4 \phi_2, 0)$, i.e. $S_1^-(P_r)$ in Fig 6. ∎
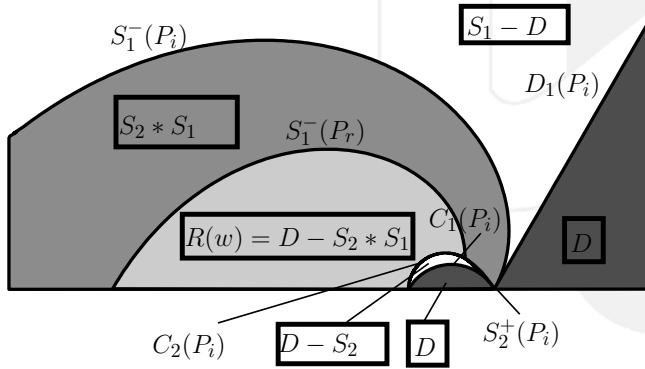

Fig. 6. Region $R(w)$ where a $w = D - S_2 * S_1$ path is shorter than the best 2−letter ones, for $r_0 = 10$ and $\phi_2 = \frac{\pi}{3}$. The region is delimited by a ϕ_1 spiral $S_1^-(P_r)$ located inside $S_1^-(P_i)$ and by the circle $C_2(P_i)$ passing through the origin. It covers a part of region IV and a part of region II. Compare this figure with Fig. 5.

C. Families of w-trajectories in region II

In region II, the shortest paths among 2−letter trajectories are of the kind $D - S_2$. Obviously, these trajectories cannot be improved as seen before with a $\alpha_M < \alpha_{LS}$ where α_{LS} is the particular angle α_M that realizes the $D - S_2$ trajectory. Hence, the function h we introduced above has to be studied in the interval $[\alpha_{LS}, \alpha_W]$. The existence of a minimum is given by exactly the same condition as above, except that this minimum angle $\hat{\alpha}_M$ has also to satisfy $\hat{\alpha}_M > \alpha_{LS}$. Hence, in region II, the w-trajectories will be shorter when

$$\begin{cases} r_f & < & r_0 \sin^4 \phi_2 e^{\frac{\alpha_f}{t_2}}, \\ \hat{\alpha}_M & > & \alpha_{LS}. \end{cases}$$

By using Eq. 9 the second condition translates first into

$$\alpha_f > \alpha_{LS} + \delta,$$

where $\delta = -2t_2 \log \sin \phi_2$. Now, by remaking that

$$r_f = r_0 \frac{\sin(\phi_2 - \alpha_{LS})}{\sin \phi_2} e^{\frac{\alpha_{LS} - \alpha_f}{t_2}} = \rho(\alpha_{LS}),$$

where one can check that ρ is strictly *decreasing* on $]0, \pi[$, the condition $\alpha_f > \alpha_{LS} + \delta$ can be said equivalent to

$$r_f = \rho(\alpha_{LS}) > \rho(\alpha_f - \delta) = r_0 \sin \phi_2 \sin(\phi_2 + \delta - \alpha_f), \tag{11}$$

which is the equation of a circle $C_2(P_i)$ going through the origin. As a consequence, in region II, w trajectories are shorter whenever

$$r_0 \sin \phi_2 \sin(\phi_2 + \delta - \alpha_f) < r_f < r_0 \sin^4 \phi_2 e^{\frac{\alpha_f}{t_2}}.$$

Hence, there is a region $R(w)$ where the w-trajectories are shorter than their 2−letter counterparts, and, because of lemma 3, it is equal to the *intersection of regions II and IV with the area under the spiral $S_1^-(P_r)$ defined by Eq. 10 and above the circle $C_2(P_i)$ defined by Eq. 11.* Note that these two curves intersect with the spiral $S_2^+(P_i)$ at $(r_0 \sin^2 \phi_2, \delta)$. We depicted it on Fig. 6 in light gray. Note that there still remain sub-regions of region II (resp. IV) where (up to now) the shortest paths remain $D - S_2$ (resp. $S_2 * S_1$). Among the regions modified w.r.t. the first partition, the one corresponding to $D - S_2$ optimal paths (in white in Fig.6) is now delimited, above, by the circle $C_2(P_i)$ and the spiral $S_2^+(P_i)$, and, below, by the circle $C_1(P_i)$.

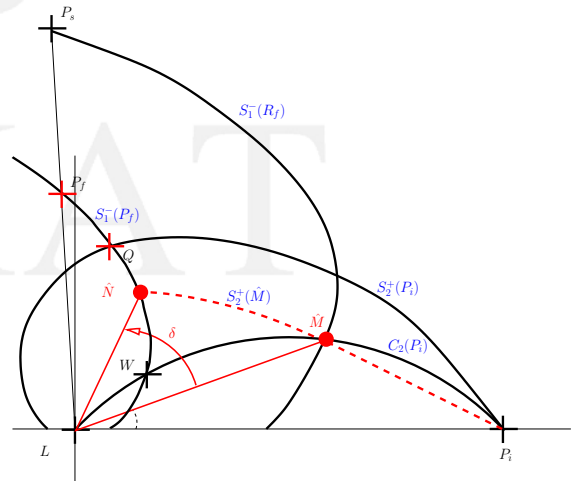### D. Geometric interpretation of the minimum

Fig. 7. Interpretation of the shortest path among the $w-$trajectories. The optimal point $\hat{M}$ is at the intersection of the arc of circle C_1 with $S_1^-(R_f)$. Moreover, the angle $\hat{M}L\hat{N}$ takes a given value, $\delta = -2t_2 \log \sin \phi_2$.

The configuration for which we reach the optimal value of the length of $w-$trajectories has some properties we describe here. First, re-writing Eq.8, one can get

$$r_0 \frac{\sin(\phi_2 - \hat{\alpha}_M)}{\sin \phi_2} = \frac{r_f}{\sin^4 \phi_2} e^{\frac{\hat{\alpha}_M - \alpha_f}{t_2}},$$

i.e. the optimal point $\hat{M}$ is to be found at the intersection of $C_1(P_i)$ (right term) with a S_1 spiral passing through the point $R_f = (\frac{r_f}{\sin^4 \phi_2}, \alpha_f)$ (left term).

Second, if one re-write the equation giving $\hat{\alpha}_N$ with the characterization of $\hat{\alpha}_M$ in Eq. 8,

$$\hat{\alpha}_N = \hat{\alpha}_M + \delta$$

where, again, $\delta = -2t_2 \log \sin \phi_2$. Among all the $w-$trajectories, the minimal length one is the one that gives this particular value δ for the angle $\hat{ML}\hat{N}$, which is a decreasing function of α_M. Hence, a necessary and sufficient condition for the value δ to be attained is that the initial value of this angle (i.e., $P_i L Q$) must be superior to δ. Not surprisingly, this condition translates exactly into Eq. 10. Both of these properties are depicted on Fig. 7.

E. 3-letter trajectories $S_2 * S_1 - D$

Similarly to w-trajectories, and by using the symmetry between P_f and P_i (one can exchange the role of the initial and final points), one can show that the $\tilde{w} = S_2 * S_1 - D$ trajectories (i) are feasible inside the regions III and IV, (ii) are better than the $2-$letter words in region IV when

$$r_f > r_0 \frac{1}{(\sin \phi_2)^4} e^{\frac{-\alpha_f}{t_2}}, \tag{12}$$

and (iii) are better than $2-$letter words in region III when

$$r_0 \frac{1}{(\sin \phi_2)^4} e^{\frac{-\alpha_f}{t_2}} < r_f < \frac{r_0}{\sin \phi_2 \sin(\phi_2 + \delta - \alpha_f)}. \tag{13}$$

This means that the region where $\tilde{w}$-trajectories are shorter than the $2-$letter trajectories is delimited, first, by the S_2 spiral $S_2^+(P_s)$ of Eq. 12, where $P_s = (r_0 \frac{1}{(\sin \phi_2)^4}, 0)$ and, second, by the half line $D_2(P_i)$ from Eq. 13. Among the regions modified w.r.t. the first partition, the one corresponding to $S_1 - D$ optimal paths (in white in Fig.9) is now delimited, on the left, by the spiral $S_1^-(P_i)$ and by the straight line $D_2(P_i)$, and, on the right, by the straight line $D_1(P_i)$.

Let us call $R(\tilde{w})$ this region and $R(w)$ its counterpart for the w-trajectories, depicted on Fig. 6. Now, inside $R(w) \cap R(\tilde{w})$, a question is: between w and $\tilde{w}$, which one is better ?

F. Which is better in the intersection ?

Let us first simplify the expression of the shortest paths in the case of $w-$ and $\tilde{w}-$trajectories. From Eq. 7, we get

$$r_N^2(\hat{\alpha}_M) = \frac{r_0 r_f \sin(\phi_2 - \hat{\alpha}_M)}{\sin \phi_2} e^{\frac{\hat{\alpha}_M - \alpha_f}{t_2}},$$

which by the characterization of the minimum leads to

$$r_N^2(\hat{\alpha}_M) = r_0^2 \sin^2 \phi_2 \sin^2(\phi_2 - \hat{\alpha}_M).$$

By using it into Eq. 6, one get

$$l(\hat{\alpha}_M) = \frac{1}{\cos \phi_2}(r_f + r_0 \cos(\hat{\alpha}_M - 2\phi_2)).$$

Symmetrically, one can show that for the optimal value $\hat{\alpha}_{M'}$ among the $\tilde{w}-$trajectories,

$$l(\hat{\alpha}_{M'}) = \frac{1}{\cos \phi_2}(r_0 + r_f \cos(\alpha_f - \hat{\alpha}_{M'} - 2\phi_2)).$$

Now it follows that the difference Δ between the lengths of the best $w-$ and $\tilde{w}-$trajectories can be expressed as a function of $\frac{r_0}{r_f}$. Indeed, by using Eq. 8 and its counterpart for $\tilde{w}-$trajectories, we get

$$\Delta(\tfrac{r_0}{r_f}) = \frac{1}{\cos \phi_2}(r_f - r_0 + r_0 \cos(\hat{\alpha}_M - 2\phi_2) \\ - r_f \cos(\alpha_f - \hat{\alpha}_{M'} - 2\phi_2)).$$

After some algebra, we get $\Delta(\frac{r_0}{r_f}) = \mu(\frac{r_0}{r_f})$, where

$$\mu(x) = \frac{r_0}{\cos \phi_2}(-1 + \frac{1}{x} + \cos(g^{-1}(x) - 2\phi_2) - \\ \frac{1}{x} \cos(g^{-1}(\frac{1}{x}) - 2\phi_2)).$$

As g is a strictly increasing function, its reciprocal function g^{-1} is also strictly increasing. The derivative of μ is

$$\mu'(x) = \frac{r_0}{\cos \phi_2}(-\frac{1}{x^2}(1 - \cos(g^{-1}(\frac{1}{x}) - 2\phi_2))) \\ - g^{-1'}(x) \sin(g^{-1}(x) - 2\phi_2) \\ - \frac{g^{-1'}(\frac{1}{x})}{x^3} \sin(g^{-1}(\frac{1}{x}) - 2\phi_2)).$$

Each term of the derivative of μ is negative, at any $x > 0$, which induces that μ is a decreasing function. Moreover, $\mu(1) = 0$, so that we can conclude that

1) if $r_0 < r_f$, Δ is positive, i.e., the best $\tilde{w}-$trajectory is *shorter* than the best $w-$trajectory,
2) if $r_f < r_0$, the best $w-$trajectory is shorter.

Hence, the boundary between the regions where $w-$trajectories are the shortest among $3-$letter trajectories, and the ones where $\tilde{w}-$trajectories are the shortest, is an arc of circle of center L, radius r_0, that we will call $C_0(P_i)$.

IV. $4-$LETTER TRAJECTORIES AS OPTIMAL PATHS

In this section, we examine 4-letter trajectories and study where in the plane they give the best way to reach P_f.

A. 4-letter trajectories $D - S_2 * S_1 - D$

First, note that the two possible $4-$letter trajectories operate each on one of the symmetric half-planes, the argument being similar as in the proof of lemma 2. Hence, we consider only $D - S_2 * S_1 - D$ trajectories, in the positive half-plane.

Now refer to Fig. 8(a), similarly to what we saw with $w-$trajectories, the family of 4-letter trajectories can be parameterized with two points M and M' located, respectively, on the two circles $C_1(P_i)$ and $\bar{C}_1(P_f)$ relative to points P_i and P_f. We will use, again, their polar angle α_M and $\alpha_{M'}$ as parameters for the $4-$letter trajectory. Note that a priori $0 < \alpha_M < \phi_2$ and $\alpha_f - \phi_2 < \alpha_{M'} < \alpha_f$.

Following the example of Section III, we first write the path length as a function of α_M and $\alpha_{M'}$
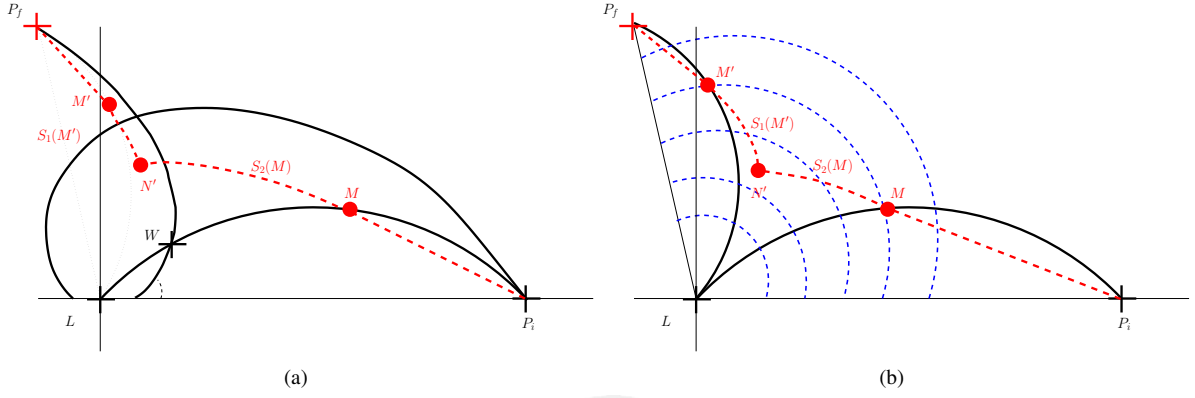
Fig. 8. In (a), construction of a $4-$letter word. In (b), construction of the optimal one. Each of the circles centered on L and of radius inferior to $\min(r_0, r_f)$ intersects the circles C_1 and $\bar{C}_1$ relative to P_i and P_f, at points M and M'. At the optimum, the angle $M'LM$, which increases with the radius of the circles, is equal to 2δ.

$$
\begin{aligned}
l(\alpha_M, \alpha_{M'}) &= P_f M' + M'N' + N'M + MP_i \\
&= r_0 \frac{\sin(\alpha_M)}{\sin\phi_2} + r_f \frac{\sin(\alpha_f - \alpha_{M'})}{\sin\phi_2} \\
&\quad + \frac{1}{\cos\phi_2}(r_M + r_{M'} - 2r_{N'}) \\
&= r_0 \frac{\cos(\alpha_M)}{\cos\phi_2} + r_f \frac{\cos(\alpha_f - \alpha_{M'})}{\cos\phi_2} - 2\frac{r_{N'}}{\cos\phi_2}.
\end{aligned}
$$

The derivation of $r_{N'}$ is easy since N' is the intersection of the S_1 spiral through M' with the S_2 spiral through M (see Fig. 8). It follows that

$$
\alpha_{N'} = \frac{1}{2}t_2 \log\frac{r_M}{r_{M'}} + \frac{1}{2}(\alpha_M + \alpha_{M'}).
$$

By using this expression in the one giving $l(\alpha_M, \alpha_{M'})$, one finally get

$$
\begin{aligned}
l(\alpha_M, \alpha_{M'}) = \quad & r_0\frac{\cos(\alpha_M)}{\cos\phi_2} + r_f\frac{\cos(\alpha_f - \alpha_{M'})}{\cos\phi_2} \\
& -2\frac{\sqrt{r_0 r_f \sin(\phi_2 - \alpha_M)\sin(\phi_2 + \alpha_{M'} - \alpha_f)}}{\sin\phi_2 \cos\phi_2}e^{\frac{\alpha_M - \alpha_{M'}}{2t_2}}.
\end{aligned}
$$

Note that in both cases $\alpha_M = 0$ or $\alpha_{M'} = \alpha_f$, we fall in the case of $3-$letter words. We are interested in finding extrema for this 2-variable function. Its partial derivatives can be calculated after some developments,

$$
\frac{\partial l}{\partial \alpha_M} = \frac{r_0 \sin\alpha_M}{\cos\phi_2}\left(-1 + \frac{1}{\sin^2\phi_2}\sqrt{\frac{r_{M'}}{r_M}}e^{\frac{\alpha_M - \alpha_{M'}}{2t_2}}\right),
$$

and

$$
\frac{\partial l}{\partial \alpha_{M'}} = \frac{r_f \sin(\alpha_f - \alpha_{M'})}{\cos\phi_2}\left(-1 + \frac{1}{\sin^2\phi_2}\sqrt{\frac{r_M}{r_{M'}}}e^{\frac{\alpha_M - \alpha_{M'}}{2t_2}}\right).
$$

Vanishing both derivatives leads to the rather simple characterizations of the shortest curves

$$
\begin{cases}
r_M &= r_{M'} \\
\alpha_M &= \alpha_{M'} - 2\delta,
\end{cases}
$$

where we use again $\delta = -2t_2 \log\sin\phi_2$.

Above all, these characterizations allow geometrical reasoning on the existence and the nature of the extremal curves. Consider Fig. 8(b), and the family of circles centered on the

origin (in dashed line). Among these circles that intersect both of the arcs of circles C_1 (resp. $\bar{C}_1$) relative to P_i (resp. P_f), one can measure the angle these intersections form with the origin. This angle is obviously an increasing function of the radius. At the optimum, this angle has to be equal to 2δ.

As a consequence, a sufficient and necessary condition to get an optimum is that, at the largest circle that can be built (i.e. with radius $\min(r_0, r_f)$), the angle must be superior to 2δ. There are three cases :

1) if $\alpha_f > 2\phi_2 + 2\delta$, the angle formed by any pair of points M and M' is necessarily superior to 2δ, so that no minimal pair $(\alpha_M, \alpha_{M'})$ can be found; the shortest path is, at the limit, a trajectory formed by tow segments joined at L, which is not doable in practice as the robot cannot go through the landmark; otherwise,

2) if $r_0 < r_f$, then the largest feasible circle is simply $r = r_0$. Its intersection with the arc $C_1(P_i)$ is P_i itself, whereas the one with the $\bar{C}_1(P_f)$ is given by

$$
r_0 = r_f \frac{\sin(\phi_2 + \alpha_{M'} - \alpha_f)}{\sin\phi_2}.
$$

The condition $\alpha'_M - \alpha_M > 2\delta$ translates into

$$
r_f \sin(\phi_2 + 2\delta - \alpha_f) < r_0 \sin\phi_2.
$$

The corresponding points form an area delimited by a straight line of angle $\phi_2 + 2\delta$ (referred to as $D_3(P_i)$ in Fig 9) and by the circle $r = r_0$.

3) if $r_f < r_0$, the largest feasible circle is $r = r_f$, which intersects the $\bar{C}_1(P_f)$ in P_f itself and the $C_1(P_i)$ at

$$
r_f = r_0 \frac{\sin(\phi_2 - \alpha_M)}{\sin\phi_2}.
$$

Then, the condition $\alpha_{M'} - \alpha_M > 2\delta$ is equivalent to

$$
r_f > r_0 \frac{\sin(\phi_2 + 2\delta - \alpha_f)}{\sin\phi_2},
$$

which says that point P_f is above an arc of circle $C_3(P_i)$ passing through the origin with a slope $\phi_2 + 2\delta$, and of radius $\frac{r_0}{\sin\phi_2}$.

B. Absence of optimal paths for large values of α_f

As stated above, when $\alpha_f > 2\phi_2 + 2\delta$, there cannot have an optimal path for the $4-$letter paths. At the limit the shortest path would be done by a not-realizable trajectory made of two segments. This trajectory is not realizable as it crosses the landmark. We can easily exhibit a family of $4-$letter path converging towards this limit trajectory, e.g.:

$$\left\{ \begin{array}{ccc} \alpha_M^{(k)} & = & \phi_2(1 - e^{-k}) \\ r^{(k)}{}_M & = & r^{(k)}{}_{M'} \end{array} \right.$$

define a family of trajectories converging as close as we want to the two-segments trajectory. As a consequence, for points located below the line $D_4(P_i)$ (see Fig. 9), there is no realizable optimal path, but a limit trajectory passing through the landmark. The equation of line $D_4(P_i)$ is $\alpha = 2\phi_2 + 2\delta$.

C. Partition of the plane among possible trajectories

By combining the results of Section III and IV, and in particular all the critical curves that separate regions where one kind of trajectory gives the shortest path, we deduce the partition of Fig. 9, that gives for any point of the plane the nature of this trajectory. Most of the plane is made of $D - S * S - D$ trajectories (in magenta), $S * S - D$ trajectories (in red), straight lines or $D - S * S$ trajectories (in yellow). Some regions still remain where $2-$letter trajectories are shorter (in cyan and blue).

V. Conclusion

We have studied in this article the spatial distribution of optimal trajectories for a system made of a differential drive robot under the constraint that some object has to remain in sight of a limited angle sensor. The distribution of the nature of shortest paths is more complex than expected, as one has to consider $3-$ and $4-$letter trajectories as possible candidates for shortest paths. We have shown that there cannot have more than four primitives in the optimal path and we have given a partition of the plane in function of the nature of these optimal paths. Our future works will focus on extending this study to more general metrics, like time-optimal trajectories and to other mechanical systems.

References

[1] D. J. Balkcom and M. T. Mason. Time optimal trajectories for bounded velocity differential drive vehicles. *Int. J. of Robotics Research*, 21(3):199–217, 2002.

[2] S. Bhattacharya, R. Murrieta-Cid, and S. Hutchinson. Optimal paths for landmark-based navigation by differential-drive vehicles with field-of-view constraints. *IEEE Trans. on Robotics*, 23(1):47–59, 2007.

[3] A.J. Briggs, C. Detweiler, D. Scharstein, and A. Vandenberg-Rodes. Expected shortest paths for landmark-based robot navigation. *Int. J. of Robotics Research*, 8(12), 2004.

[4] H. Chitsaz, S.M. LaValle, D.J. Balkcom, and M.T. Mazon. Minimum wheel-rotation paths for differential-drive robots. In *IEEE Int. Conf. on Robotics and Automation*, pages 1616–1623, 2006.

[5] J. B. Hayet, F. Lerasle, and M. Devy. A visual landmark framework for mobile robot navigation. *Image and Vision Computing*, 8(25):1341–1351, 2007.

[6] J.B. Hayet, C. Esteves, and R. Murrieta-Cid. A motion planner for maintaining landmark visibility with a differential drive robot. In *Workshop on Algorithmic Foundations of Robotics*, 2008.

[7] J.-P. Laumond, P. E. Jacobs, M. Taïx, and R. M. Murray. A motion planner for nonholonomic mobile robots. *IEEE Trans. on Robotics and Automation*, 10(5):577–593, 1994.

[8] G. López-Nicolás, S. Bhattacharya, J.J. Guerrero, C. Sagüés, and S. Hutchinson. Switched homography-based visual control of differential drive vehicles with field-of-view constraints. In *Proc. of the IEEE Int. Conf. on Robotics and Automation*, pages 4238–4244, 2007.

[9] J. Reeds and L. Shepp. Optimal paths for a car that goes both forwards and backwards. *Pacific J. of Mathematics*, 145(2):367–393, 1990.

[10] P. Salaris, F. Belo, D. Fontanelli, L. Greco, and A. Bicchi. Optimal paths in a constrained image plane for purely image-based parking. In *IEEE/RSJ Int. Conf. on Intelligent Robots and Systems*, 2008.

[11] P. Souères and J.-P. Laumond. Shortest paths synthesis for a car-like robot. *IEEE Trans. on Automatic Control*, 41(5):672–688, May 1996.

[12] S. Thrun. Bayesian landmark learning for mobile robot localization. *Machine Learning*, 33(1), Oct 1998.
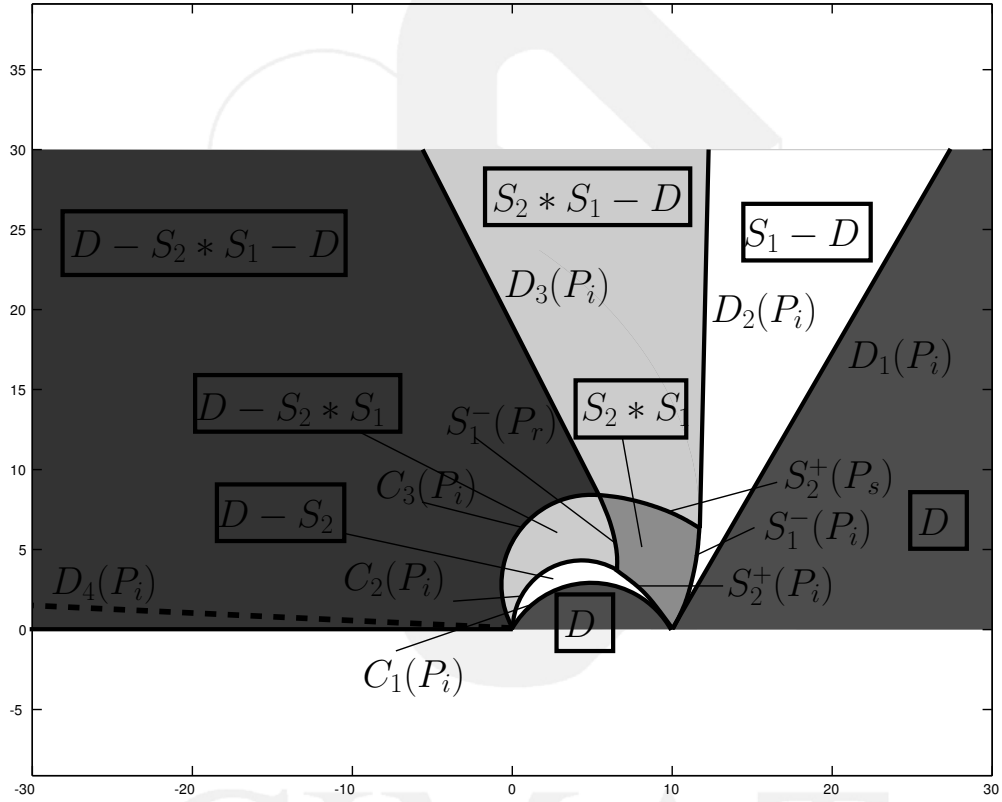
Fig. 9. Partition of the plane according to the nature of the shortest trajectory among all possible trajectories for the DDR under visibility and sensor constraints. The darkest region is the one where $4-$letter trajectories are shorter. The second darkest region is the one where line segments are shorter. White areas correspond to $S_1 - D$ or $D - S_2$ trajectories, other levels of grays correspond to $S_2 * S_1$ trajectories, and $3 - letter\ S_2 * S_1 - D$ and $D - S_2 * S_1$ trajectories. In the area below $D_4(P_i)$, the theoretical optimal is not realizable, but we can realize curves as close as we want of this optimal.